

AD-A093 089

HOWARD UNIV WASHINGTON D C DEPT OF CHEMISTRY

F/6 7/4

RAMAN INVESTIGATION OF OPTICAL FIBERS UNDER HIGH TENSILE STRESS--ETC(U)

NOV 80 G E WALRAFEN, P N KRISHNAN

N00014-80-C-0305

UNCLASSIFIED

TR-1

NL

1 of 1
AD-A093 089

END
DATE
FILMED
2-81
DTIC

AD A093089

LEVEL

(2)

OFFICE OF NAVAL RESEARCH

N00014-80-C-0305

Task No. NR 051-733

TECHNICAL REPORT NO. 1

RAMAN INVESTIGATION OF OPTICAL FIBERS

UNDER HIGH TENSILE STRESS

by

G. E. Walrafen
Department of Chemistry
Howard University
Washington, D. C. 20059

P. N. Krishnan
Department of Chemistry
Coppin State College
Baltimore, Maryland 21216

and

S. W. Freiman
National Bureau of Standards
Gaithersburg, Maryland 20834

DTIC
ELECTE
DEC 19 1980

in press

at the

Journal of Applied Physics

November 25, 1980

Reproduction in whole or in part is permitted for
any purpose of the United States Government

This document has been approved for public release
and sale; its distribution is unlimited

*Presented at the 82nd annual meeting of the American Ceramic Society,
Chicago, Illinois, April 29, 1980.

80 12 19 085

DDC FILE COPY

Unclassified

SECURITY CLASSIFICATION OF THIS PAGE (When Data Entered)

REPORT DOCUMENTATION PAGE		READ INSTRUCTIONS BEFORE COMPLETING FORM
1. REPORT NUMBER 1	2. GOVT ACCESSION NO. AD-A093 089	3. RECIPIENT'S CATALOG NUMBER
4. TITLE (and Subtitle) Raman Investigation of Optical Fibers Under High Tensile Stress.		5. TYPE OF REPORT & PERIOD COVERED Technical Report, #1 1980
7. AUTHOR(s) G. E. Walrafen, P. N. Krishnan and S. W. Freiman		6. PERFORMING ORG. REPORT NUMBER
9. PERFORMING ORGANIZATION NAME AND ADDRESS Howard University Department of Chemistry Washington, D.C. 20059		8. CONTRACT OR GRANT NUMBER(s) N00014-80-C-0305
11. CONTROLLING OFFICE NAME AND ADDRESS Office of Naval Research Arlington, VA 22217		10. PROGRAM ELEMENT, PROJECT, TASK AREA & WORK UNIT NUMBERS NR051-733
14. MONITORING AGENCY NAME & ADDRESS (if different from Controlling Office) TR-1		12. REPORT DATE November 1980
16. DISTRIBUTION STATEMENT (of this Report) Approved for Public Release; Distribution Unlimited		13. NUMBER OF PAGES 28
17. DISTRIBUTION STATEMENT (of the abstract entered in Block 20, if different from Report)		15. SECURITY CLASS. (of this report) Unclassified
18. SUPPLEMENTARY NOTES Accepted for publication in the Journal of Applied Physics		15a. DECLASSIFICATION/DOWNGRADING SCHEDULE
19. KEY WORDS (Continue on reverse side if necessary and identify by block number) Optical Fibers Fused Silica Raman Spectroscopy		
20. ABSTRACT (Continue on reverse side if necessary and identify by block number) → Raman spectra have been obtained from fused silica optical fibers under tensile stresses from 0 to 3.3 GPa (33 kbar). Reversible intensity increases relative to the principal Raman maximum at 490 cm^{-1} were observed for the defect peak at 490 cm^{-1} and for shoulders near 350-375 cm^{-1} and 115 cm^{-1} . Application of tensile stress to fused silica appears to produce changes in the stretched Si—O defect sites, as well as changes in the main network structure.		

DD FORM 1 JAN 73 1473

EDITION OF 1 NOV 65 IS OBSOLETE
S/N 0102-014-6601

SECURITY CLASSIFICATION OF THIS PAGE (When Data Entered)

171660

(1)

"Raman Investigation of Optical Fibers
Under High Tensile Stress" *

by

G. E. Walrafen
Department of Chemistry
Howard University
Washington, D. C. 20059

P. N. Krishnan
Department of Chemistry
Coppin State College
Baltimore, Maryland 21216

and

S. W. Freiman
National Bureau of Standards
Gaithersburg, Maryland 20234

* Presented at the 82nd annual meeting of the American
Ceramic Society, Chicago, Illinois, April 29, 1980.

Accession For	
NTIS GRA&I	
DTIC TAB	
Unannounced	
Justification	
By	
Distribution/	
Availability Codes	
Dist	Avail and/or Special
A	

(2)

ABSTRACT

Raman spectra have been obtained from fused silica optical fibers under tensile stresses from 0 to 3.3 GPa (33 kbar). Reversible intensity increases, relative to the principal Raman maximum at 490 cm^{-1} were observed for the defect peak at 490 cm^{-1} and for shoulders near $350\text{-}375\text{ cm}^{-1}$ and 115 cm^{-1} . Application of tensile stress to fused silica appears to produce changes in the stretched Si—O defect sites, as well as changes in the main network structure.

INTRODUCTION

Raman features from fused silica near 490 and 604 cm^{-1} have been examined in several recent investigations,^(1 - 7) see Fig. 1 (stars). Raman intensities at 490 and 604 cm^{-1} were found to increase with increasing fictive temperature, T_F , when the OH content was constant (or zero).⁽⁴⁾ The 490 and 604 cm^{-1} Raman intensities were also observed to decrease with increasing OH content, at constant T_F .⁽⁴⁾ In the latter case, a weak Raman band near 970 cm^{-1} due to Si versus OH stretching,^(4,8) was produced at the expense of intensity at the 490 and 604 cm^{-1} positions. Other findings, such as the observation that the 490 and 604 cm^{-1} intensities from samples having high T_F 's could be reduced by annealing, strengthened the hypothesis that these peaks could be assigned to defects in the silica structure.⁽⁴⁾

The nature of the above defects suggested that their concentration and/or molar intensity should increase under the application of tensile stress. In order to subject a sufficient volume of glass to large tensile stresses,⁽⁹⁾ experiments were conducted on glass optical fibers. An interpretation of the changes observed in the Raman spectrum is presented in terms of variations in the Si—O binding at defect sites.

EXPERIMENTAL PROCEDURES

Pure fused silica optical fibers were used in all experiments (silicone rubber cladding, 200 μ m diameter),⁽¹⁰⁾ The OH content of the fibers was about 530 ppm,⁽¹¹⁾ and T_F values were estimated to be roughly 1700 - 1800° C.⁽¹²⁾ The constancy of the OH concentration was assured by monitoring the Raman OH-stretching intensity near 3700 cm^{-1} ⁽¹³⁾

Forward scattered Raman spectra were obtained by focussing the fiber output on the entrance slit of an Instruments S. A. HG2S holographic grating double monochromator, Fig. 2. Raman excitation was accomplished using 514.5 nm argon ion laser radiation at about 0.6 W. Slit-widths ranged from 2 to 3 cm^{-1} and detection was accomplished with an uncooled Hamamatsu R928 PM tube, a Keithley 414S picoammeter, and a high-speed Esterline Angus L1101S recorder.

Load was applied to the fiber by suspending a weight from a clamp near the end of the fiber, Fig. 2. The optical fiber was held by strips of sponge rubber placed between wooden strips 30 to 50 cm in length, tightly clamped together in several places. This arrangement prevented any slippage during application of load. The stressed-to-unstressed length ratio was maintained in the range of 5 to 50 to reduce the unstressed spectral contribution.

Some Raman experiments were also attempted in which only stressed fiber was examined by focussing 90 degree scattered radiation on the slit, but these experiments were abandoned because the S/N (signal-to-noise) ratio, although good, was

at least 20-fold lower than that obtained from forward Raman scattering.

Because the Raman depolarization ratio varies across the fused silica spectrum,⁽¹⁴⁾ it was necessary to determine if the polarization, which is ordinarily scrambled by an optical fiber, changes under tensile stress. Preliminary experiments involved examination of the mode structure and the polarization at the fiber output. No significant changes were observed in the high-order mode structure under stress, and no changes whatever in polarization were detected using polarizers or crossed polarizers.

Quantitative measurements of the polarization were made using the optical fiber emission to excite both forward and 90 degree Raman scattering in liquid CCl_4 . Ratios of integrated Raman intensities were determined for the CCl_4 peaks at 218(dp), 314(dp), and 459(p) cm^{-1} (Here dp refers to a depolarization ratio of 0.75 and p to a ratio of about 0.01⁽¹⁵⁾.) For both forward and 90 degree scattering, no changes whatever were detected in the intensity ratios I_{459}/I_{314} and I_{459}/I_{218} for tensile stresses to 2.19 GPa. Further, the intensity ratios obtained from CCl_4 were those characteristic of unpolarized excitation, as expected from the fact that polarization is scrambled by internal reflection in high-mode optical fibers. Also, it should be emphasized that the above integrated Raman intensity ratios from CCl_4 constitute a particularly sensitive

(6)

test of the polarization properties of the exciting radiation
emitted from the optical fiber.

RESULTS

Stressed and unstressed Raman spectra illustrative of the approximately 50 individual experiments performed are shown in Fig. 1. The (upper) spectrum was taken at a tensile stress of 3.34 GPa (33.4 kbar), while the lower spectrum was taken from an unstressed fiber. The intensification of the 490 cm^{-1} defect peak (starred), relative to the 440 cm^{-1} peak, is visually obvious, and is emphasized by the horizontal lines. In the unstressed spectrum, the 490 and 440 cm^{-1} peaks occur at the same vertical height, as seen by the horizontal line through them, but at 3.34 GPa (upper) the 490 cm^{-1} peak height is well above the horizontal line. Similar conclusions may be drawn from examination of the inset of Fig. 1, which refers to three spectra run in the sequence unstressed, U; stressed at 2.19 GPa, S; and, relaxed, R, with 20-30 min between spectra.⁽¹⁶⁾

The visual observation that the 490 cm^{-1} peak height increases relative to the 440 cm^{-1} peak height, i.e., that I_{490}/I_{440} increases, may mean either that I_{490} increased at constant I_{440} , or that I_{440} decreased at constant I_{490} , or that both I_{490} and I_{440} changed, or even that more complicated changes occurred, such as broadening, etc. Hence, if I_{440} is to be regarded as a reference standard, it is desirable to understand how I_{440} varies relative to other peaks, such as the intense peak at 60 cm^{-1} .

Peak heights above baseline A, Fig. 1, were measured for the 60, 440, and 800 cm^{-1} peaks at a series of tensile stresses. Consistency of drawing baseline A under all spectra was obtained by using a single template whose shape, baseline A, Fig. 1, was determined through repeated trials. The template was positioned to a given Raman spectrum by simultaneously matching two regions: 1) the region between the exciting line and the sharp minimum near 20 to 25 cm^{-1} and, 2) the region from about 900-1000 cm^{-1} . The results are shown in Table I in terms of the ratios I_{60}/I_{440} , I_{800}/I_{440} , and I_{800}/I_{60} .

The average value for the peak height ratio I_{60}/I_{440} from Table I is 0.70 ± 0.02 , which within present errors is constant. Similarly, the ratios I_{800}/I_{440} and I_{800}/I_{60} are also seen to be constant, Table I. The constancy of the ratio I_{60}/I_{440} is particularly important because the peaks at 60 and 440 cm^{-1} have both the largest peak heights, and the highest integrated intensities (Fig. 1) in the fused silica spectrum.

Quantitative values of peak height ratios are often difficult to obtain accurately when weak features such as at 490 and 604 cm^{-1} are involved, because such ratios suffer from errors in baseline estimates, and peak S/N ratios. Peak height ratios also ignore component broadening. A better method is to use ratios of integrated intensities. For the 490 and 604 cm^{-1} peaks, Fig. 1, integrated intensities may be obtained using baseline B. Baseline B was obtained by using a French curve. In contrast,

(9)

an integrated intensity for the 440 cm^{-1} component could not be readily obtained, because the component shape is unknown. Therefore, the total integrated Raman intensity from about 20 to 900 cm^{-1} was obtained using baseline A, minus, of course, the contributions from the 490 and 604 cm^{-1} components. The resulting ratios of integrated Raman intensities, I_{490}/I_T and I_{604}/I_T , where T refers to the total Raman area, minus the 490 and 604 cm^{-1} component areas, are shown for tensile stresses from 0 to 2.19 GPa in Table II. In addition, the quantities I_{490}/I_{440} and I_{604}/I_{440} are listed in the Table, where I_{490} and I_{604} are integrated intensities above baseline B, and I_{440} refers to the peak height above baseline A. The latter ratios were used in Table II because of the intensification of shoulders described subsequently. It should also be made very clear that the 490 cm^{-1} component area (the integrated component intensity) obtained above baseline B, is independent of effects due to broadening of the 440 cm^{-1} component. Slight broadening of the 440 cm^{-1} component was clearly evident from changes in the shape of baseline B under the 490 cm^{-1} peak, but this broadening effect was completely negated by use of baseline B.

It is apparent from Table II, that the only significant changes involve the 490 cm^{-1} component, as previously suggested from examination of Fig. 1. The original data leading to Table II (using three figures, instead of the two significant figures of the Table) were treated by linear least squares. Changes of about 62% in I_{490}/I_T , and of about 67% in I_{490}/I_{440} , resulted for stresses to 2.19 GPa, using the least squares estimates, but changes in the ratios involving the 604 cm^{-1} component were not significant (negligible). Because the relative 604 cm^{-1} intensity did not change with tensile stress, it can be concluded from Tables I and II that

Raman intensities at 60, 440, 604, and 800 cm^{-1} are either all independent of, or vary in the same way with, tensile stress.

In addition to relative intensification of the 490 cm^{-1} peak, other small spectral changes were seen for Raman features below 440 cm^{-1} . One effect which occurred consistently throughout this work is an apparent enhancement under tensile stress of a shoulder near 350-375 cm^{-1} evident from careful examination of Fig. 1, particularly the inset. In the inset, the region from about 440 cm^{-1} to 350 cm^{-1} has the same slope in both the U and R spectra. However, this slope is smaller for the S spectrum, indicating a slight intensification of the 350-375 cm^{-1} shoulder component. However, the 350-375 cm^{-1} shoulder would also appear to intensify, if the 440 cm^{-1} component broadened. Experience with baseline B at high tensile stress indicates a slight but definite broadening of the 440 cm^{-1} component, which could account for part (or all) of the intensification at 350-375 cm^{-1} . In regard to intensification due to broadening of neighboring components, it should be emphasized ^{again} that the relative intensification at 490 cm^{-1} cannot be so explained, because the 440 cm^{-1} broadening is subtracted from the integrated intensity at 490 cm^{-1} by virtue of curvature in baseline B, Table II.

Some shape changes may also occur in the Raman region between 0 and 200 cm^{-1} under increasing tensile stress. A shoulder at roughly $115 \pm 5 \text{ cm}^{-1}$ appears to be more prominent under high stress, compared to the nominal 60 cm^{-1} intensity maximum, Fig. 1. The Raman amplitude ratio, I_{115}/I_{60} , using the method A baseline, increases roughly 5% in the figure. The position of the Raman peak at 60 cm^{-1} seemed not to rise in position significantly, however. For tensile stresses from 0 to 2.19 GPa, the position ranged from 60 ± 2 to $63 \pm 2 \text{ cm}^{-1}$ i.e., about constant. However, it was not possible to determine whether or not the relative intensification at 115 cm^{-1} resulted from an increasing half-width of the 60 cm^{-1} component.

DISCUSSION

Three distinct types of behavior have now been delineated in regard to the intensity variations of the 490 and 604 cm^{-1} peaks from fused silica as follows: 1) intensity increases at both the 490 and 604 cm^{-1} positions with increasing T_P ,⁽⁴⁾ 2) a large intensity increase at 604 cm^{-1} relative to the 490 cm^{-1} peak observed when fused silica is densified by neutron irradiation,⁽²⁾ and 3) the reversible Raman intensity increase at 490 cm^{-1} observed here. It should be emphasized, however, that the type 1 and 2 variations differ markedly from the type 3 variation--annealing is required to produce reversibility for types 1 and 2.

In previous Raman work,⁽²⁻⁴⁾ lines near 490 and 604 cm^{-1} were assigned to defects of the type $\text{—Si—O}\cdots\text{Si—}$, where the dots refer to a broken bond. However, in view of the EPR inactivity of ordinary bulk fused silica,⁽¹⁷⁾ it is more appropriate to think of the defect as a stretched bond, or related to the effects of a stretched bond. Such a stretched bond would have a smaller force constant, i.e., would be dynamically weakened, but would certainly not be broken from an energetic point of view, that is, it would not be a point defect in the usual sense. Such a "defect" could be considered as a Si—O bond associated with a small (e.g., less than 120°) bridging bond angle, and consequently with a large (e.g., greater than 1.68 Å) Si—O bond length.⁽¹⁸⁾

In regard to a decreased force constant, no significant frequency shifts were observed in this work, and in previous Raman work,⁽⁴⁾ for the defect lines at 490 and 604 cm^{-1} . Also the shifts reported for the defect lines by Bates et al.⁽²⁾ are 2% or less. Thus, the 490 and 604 cm^{-1} lines probably refer to vibrational modes affected by, but not directly related to, the Si—O elongation involved. Further, the 490 and 604 cm^{-1} Raman lines are unusually sharp for glasses. Thus, it is not unreasonable to relate these lines to local modes decoupled from the silica network by virtue of a stretched Si—O bond, e.g., modes of the O_3Si or OSiO_3 units and/or of the $\text{O}_3\text{Si—OSiO}_3$ grouping, in which one intervening and elongated Si—O bond replaces the dots in the previous —Si—O···Si— picture. Because the concentration of stretched Si—O bonds may be only about $6 \times 10^{19}/\text{cm}^3$ ^(4,19) or about 0.1%, a significant lowering of the stretching frequency at 1060 cm^{-1} would not be expected, that is, most of the Si—O vibrations correspond to the main glass structure.

In previous Raman studies of fused silica, it was estimated that a small fraction, roughly $6 \times 10^{19}/\text{cm}^3$ ⁽⁴⁾ of defects, for example, of highly elongated Si—O bonds might exist. This high-energy fraction would be "frozen" into the thermodynamically unstable structure that is produced by rapid quenching. Because such elongated bonds would constitute high-energy sites, they would probably react preferentially with water to form adjacent Si—OH groups.⁽¹³⁾ Further, high tensile stress might also increase the fraction of

elongated Si—O bonds. Or, high tensile stress could alter structures immediately associated with the elongated bonds, i.e., the effects of temperature rise and of tensile stress could be very different mechanistically. At any rate, the defects envisioned here are topological network defects associated with elongated high-energy Si—O bonds whose concentrations may be changed by changes in T_F , or alternatively through preferential chemical reaction with H_2O ,^(3,4) GeO_2 or B_2O_3 ,⁽³⁾ etc.

It should also be mentioned that when uniaxial stress is applied to fused silica, changes such as the intensification of Raman shoulders at $350-375\text{ cm}^{-1}$ and at $115 \pm 5\text{ cm}^{-1}$ occur, along with the intensity increases at 490 cm^{-1} . Apparently, the main silica network suffers reversible distortions, as well as the reversible bond elongations related to the defects. The intensifications of Raman shoulders observed here are significant, and do not appear to have been observed previously.

The magnitude of the intensity changes observed in the tensile stress experiments can be shown to be surprisingly large compared to the energy imparted to the fused silica optical fiber by virtue of the work done in stretching it. Our measurements indicate that a 7 kg weight, when suspended from a fiber $200\text{ }\mu\text{m}$ in diameter (tensile stress, 2.19 GPa) and 447 cm long, stretches the fiber about 12.7 cm. The work done is thus $0.41\text{ kcal/mole SiO}_2$, or $14.8\text{ cal/cm}^3\text{ SiO}_2$. This work amounts to only 0.2% of the standard heat of formation of SiO_2 glass at 25°C , ($\Delta H_f^\circ = 202.5\text{ kcal/mole SiO}_2^{(20)}$), and thus it is 10^{-3} times smaller than the Si—O bond energy. (The Si—O bond energy may be crudely approximated by dividing the ΔH_f° by 4, because

there are 4 Si—O bonds per stoichiometric SiO_2 .) However, if the defects involve stretched, rather than broken bonds, and the energy due to stretching goes disproportionately into the defect sites, the effect would be non-negligible. In this regard, the following calculation, although forced, is instructive.

Consider that the defect concentration is roughly $6 \times 10^{19}/\text{cm}^3$ (4) and that this concentration increases 60-70 % due to tensile stress, as might be inferred from the increase in the I_{490}/I_{440} ratio (Table II). Then the change in the defect concentration would be about $4 \times 10^{19}/\text{cm}^3$. Because there are 4 Si—O bonds per stoichiometric SiO_2 , the total concentration of Si—O bonds is about $9 \times 10^{22}/\text{cm}^3$, which means that the fraction changed by stretching would be 4×10^{-4} . The product of the work, about $15 \text{ cal}/\text{cm}^3$, times 4×10^{-4} is $0.01 \text{ cal}/\text{cm}^3$, which would be the energy imparted by equipartition to the new defects contained in 1 cm^3 . Because this amount of energy seems negligibly small, and the Raman intensity change at 490 cm^{-1} is visually obvious, a disproportionate amount of the work of stretching might go into creating new defects. The remaining energy, which certainly is most of the work of stretching, would go into the main silica network, as evidenced by shape changes near $350\text{-}375 \text{ cm}^{-1}$ and 115 cm^{-1} . Alternatively, because T_F is constant during stretching, a small fraction of the work of stretching could go into stretching the existing temperature-induced defects even farther, as opposed to creating new defects. This additional stretching could produce structural changes which result in matrix element effects leading to increased intensity at 490 cm^{-1} . Unfortunately, this alternative

process, although almost certainly more realistic than one involving production of additional new defects, is virtually impossible to approximate energetically at this time.

Finally, with regard to mechanistic differences between fictive temperature and uniaxial tensile stress, the reversible nature of the present experiments should be strongly emphasized. For example, annealing is required to remove the neutron-induced "defects" which give rise to greatly increased Raman intensity at 604 cm^{-1} (2) Whereas, with application of tensile stress, the Raman spectral changes are reversible ^{within} 20-30 minutes, (16) (although the actual relaxation times, which are probably very short compared to 20 minutes, have not been measured. (16)) Further, the present relaxational behavior may also be contrasted to the situation in which qualitatively similar Raman intensity changes in the 490 and 604 cm^{-1} defect components resulted for samples having T_f values of 1400°C , after annealing for 200 hr at 1100°C . (4) Hence, the presently observed reversibility is in accord with a bond stretching mechanism, whereas bond breaking or the production of new defects would probably be irreversible at room temperature.

SUMMARY AND CONCLUSIONS

The results of a new type of experiment are presented in which high tensile stress is applied to a long fused silica optical fiber while simultaneously obtaining its Raman spectrum by forward scattering. Intensification of a sharp Raman peak near 490 cm^{-1} was observed with increasing tensile stress, and the reversible nature of the intensification contrasts with previous Raman observations in which annealing was required to produce reversibility. The Raman intensification was interpreted in terms of a decoupled local mode resulting from a stretched Si—O defect site.

ACKNOWLEDGEMENTS

D. R. Hardison, Jr. and M. I. Bell are to be thanked for generous assistance in the early phases of this investigation. Numerous helpful discussions and comments on the manuscript by A. G. Revesz and R. H. Stolen are greatly appreciated. The work was funded by ONR contracts at the National Bureau of Standards and at Howard University (laser-Chemistry). The Raman instrument employed in this work was purchased through a grant from the National Science Foundation, Chemical Thermodynamics Program, CHE77-09888. Samples of high-strength optical fibers were kindly supplied by C. R. Kurkjian.

NOTE ADDED IN PROOF

Raman experiments have recently been conducted of the rate of increase of the OH-stretching peak intensity at 3700 cm^{-1} relative to the 800 cm^{-1} silica peak intensity, for a silicone rubber clad fused silica optical fiber, with and without tensile stress. To stresses of 1.56 GPa, no significant increase in the rate of the OH-stretching intensity, above the slow rise characteristic of the water uptake of the unstressed fiber, could be detected. Thus, the reversible increase in the 490 cm^{-1} peak intensity observed in this work, and the lack of a corresponding effect on the rate of water uptake, contrasts with the decreased intensity observed at 490 and 604 cm^{-1} when the OH content increases at constant T_F .⁽⁴⁾ It would appear, therefore, that no additional chemically active sites result when increased tensile stress is applied to a fused silica fiber. On the contrary, it now seems that the 490 cm^{-1} intensification is a matrix element effect associated with a structural change in existing defects. The Raman experiments involving the rate of water uptake will be described more fully elsewhere.

REFERENCES

1. R. H. Stolen, J. T. Krause, and C. R. Kurkjian, Discuss. Faraday Soc. 50, 103(1970).
2. J. B. Bates, R. W. Hendricks, and L. B. Shaffer, J. Chem. Phys. 61, 1910(1974).
3. G. E. Walrafen and J. Stone, Appl. Spectrosc. 29, 337(1975).
4. R. H. Stolen and G. E. Walrafen, J. Chem. Phys. 64, 2623(1976).
5. F. L. Galeener, J. C. Mikkelsen, Jr. and N. M. Johnson, "The Physics of SiO₂ and Its Interfaces" Pergamon, New York, 1978, p. 284.
6. J. C. Mikkelsen, Jr. and F. L. Galeener, J. Noncryst. Solids 37, 71(1980).
7. F. R. Aussenegg, M. E. Lippitsch, E. Schieffer, U. Deserno, and D. Rosenberger, Appl. Spectrosc. 32, 588(1978).
8. C. M. Hartwig and L. A. Rahn, J. Chem. Phys. 67, 4260(1977).
9. Initial attempts to obtain the Raman spectrum of a large stressed volume of fused silica involved examination of crack tips, see abstract of talk at 81st Annual Meeting, American Ceramic Society, Cincinnati, Ohio, Apr 29 - May 2, 1979.
10. Optelecom, Gaithersburg, Md.
11. The value of 530 ppm OH was obtained by comparing the peak height ratio, I_{3700}/I_{440} , from a fiber of known OH content, with the corresponding ratio from the fibers studied here.
 I_{3700} refers to the Raman intensity of the OH peak at 3700 cm.⁻¹
 I_{440} refers to the intensity of the principal Raman peak from fused silica.

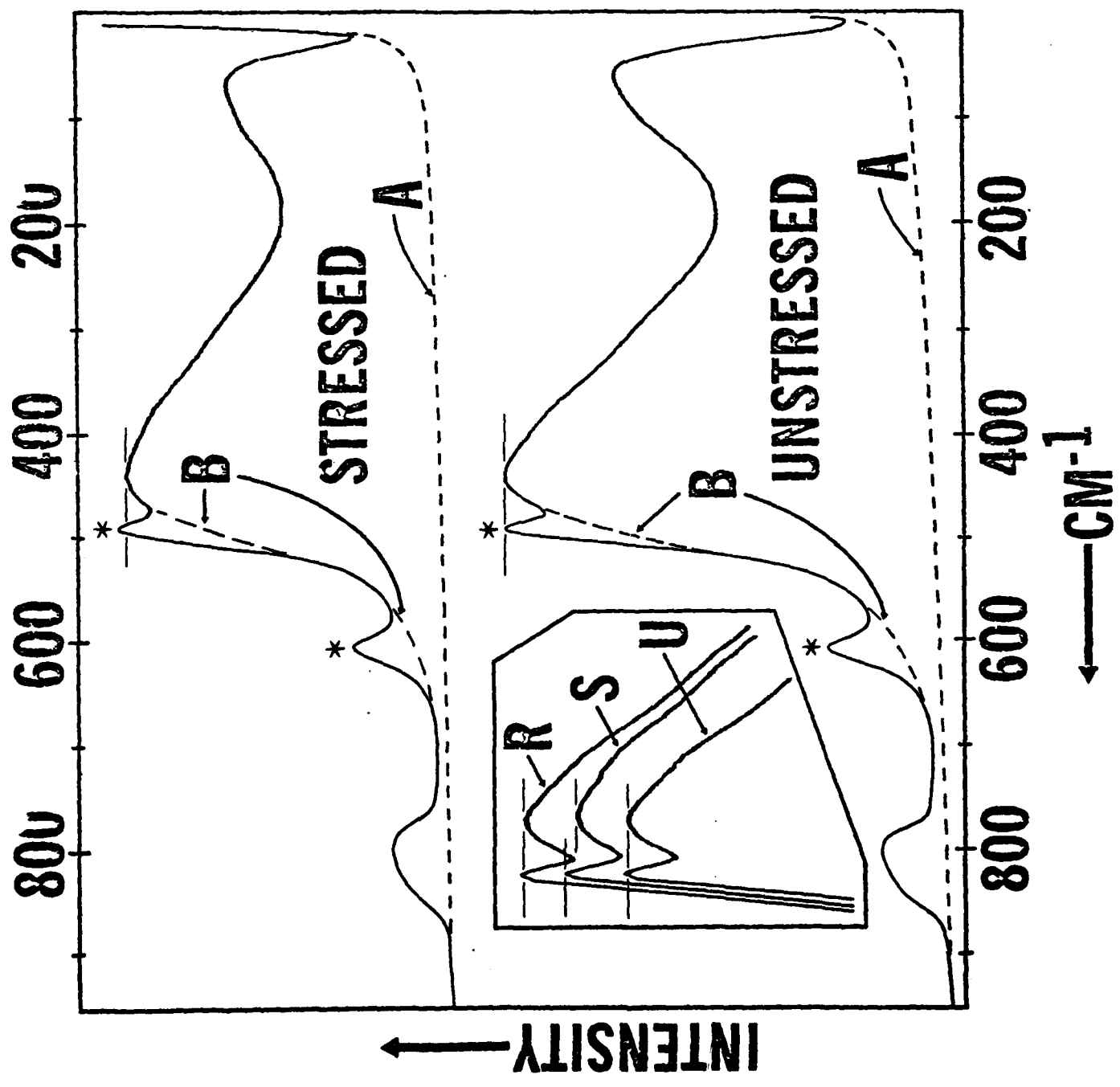
REFERENCES CONTINUED

12. T_F values were estimated by comparing the Raman peak height ratio, I_{490}/I_{440} , from fused silica of known T_F , with the corresponding ratio from the optical fibers studied here.
13. G. E. Walrafen, J. Chem. Phys. 62, 297(1975), and G. E. Walrafen and S. R. Samanta, J. Chem. Phys. 69, 493(1978).
14. M. Hass, J. Phys. Chem. Solids 31, 415(1970).
15. D. A. Long, "Raman Spectroscopy," McGraw-Hill, New York, 1977, p. 143.
16. The relaxation time is undoubtedly very much shorter than the 20 to 30 minutes required to obtain a Raman spectrum between 0 and 1100 cm^{-1} . A possible method for measuring this relaxation time by Raman techniques involves monitoring the 490 and 440 cm^{-1} peak height ratio as a function of the stretching frequency applied to the fiber by a transducer.
17. R. A. Weeks and E. Sonder, "Paramagnetic Resonance. Vol. II." Academic Press, New York, 1963, p. 869.
18. R. G. Hill and G. V. Gibbs, Acta Cryst. B35, 25(1979).
19. A. G. Revesz and G. V. Gibbs, Proceedings of the Conference on the Physics of MOS Insulators, Raleigh, NC, June 1980, G. Lucovsky et al. editors, Pergamon Press, NY, P. 92.
20. Handbook of Chemistry and Physics, R. C. Weast, editor, The Chemical Rubber Co., Cleveland, 52nd edition, 1971-72, p. D-69.

CAPTION

Fig. 1. Forward Raman scattering from fused silica optical fiber stressed to 3.34 GPa (upper), and unstressed (lower). Spectra in the inset were obtained in the sequence unstressed, U; stressed to 2.19 GPa, S; and, relaxed, R. Note that the inset spectra have been moved to the left--their position does not correspond to the cm^{-1} values below them. Baselines A and B are shown by dashes.

Fig. 1.



CAPTION

Fig. 2. Schematic illustration of method used to obtain forward Raman spectra from an optical fiber while applying tensile stress.

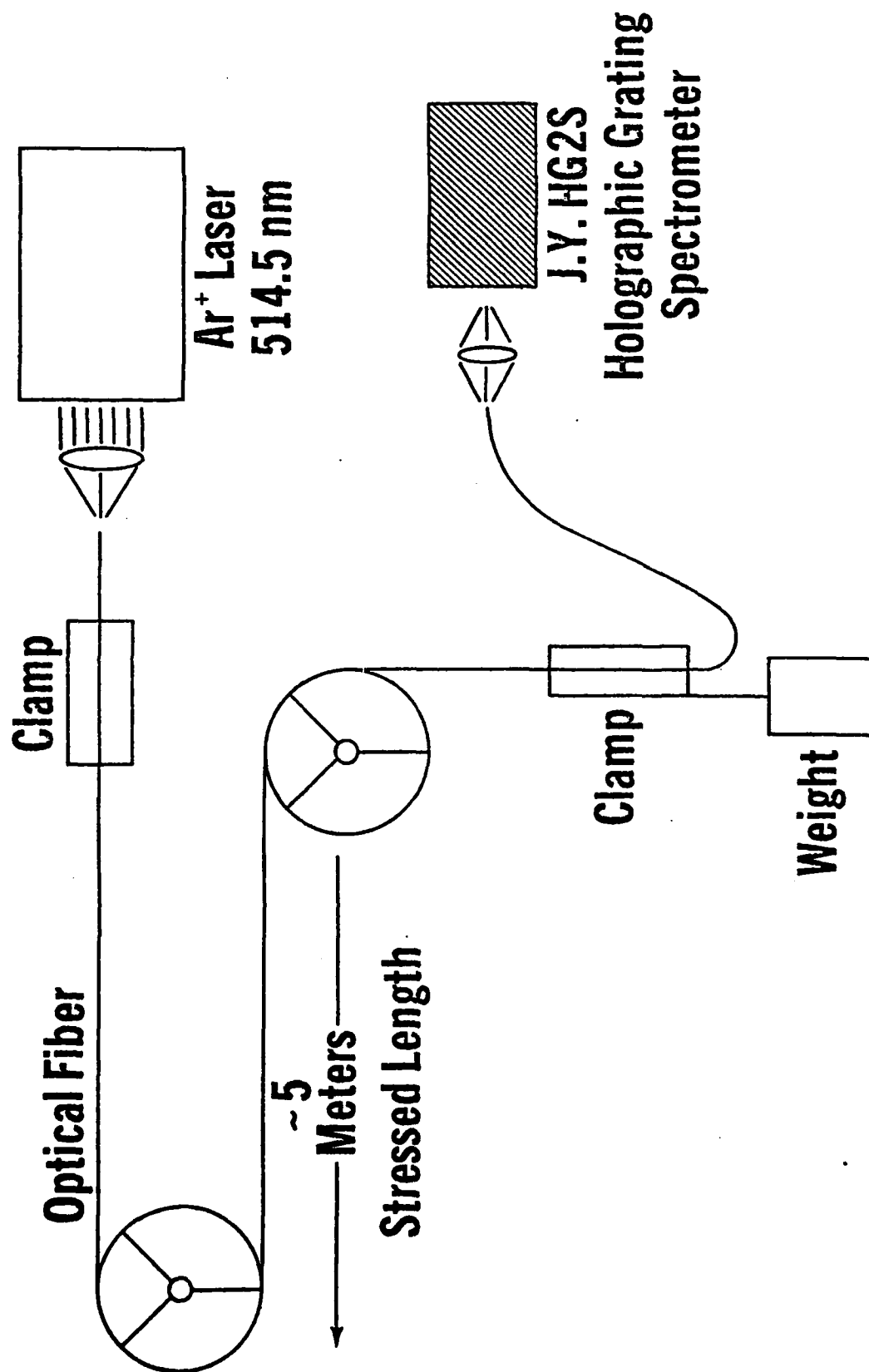


FIG. 2

CAPTION

Table I. Raman peak height ratios (I refers to peak height) for the 60, 440, and 800 cm^{-1} peaks from fused silica for tensile stresses to 2.19 GPa.

TABLE I

Stress	I_{60}/I_{440}	I_{800}/I_{440}	I_{800}/I_{60}
0 GPa	0.68	0.17	0.25
0.31	0.69	0.17	0.24
0.62	0.69	0.17	0.25
0.94	0.71	0.17	0.24
1.25	0.72	0.17	0.24
1.56	0.71	0.18	0.25
1.87	0.67	0.17	0.26
2.19	0.71	0.18	0.25

CAPTION

Table II. Ratios of integrated Raman intensities and peak heights for the 440, 490, and 604 cm^{-1} peaks from fused silica. I_{490} and I_{604} refer to integrated component intensities above baseline B, Fig. 1. I_T is the total integrated intensity above baseline A, minus the 490 and 604 cm^{-1} component areas above baseline B. I_{440} is the peak height above baseline A at 440 cm^{-1}

TABLE II

Stress	I_{490}/I_T	I_{604}/I_T	I_{490}/I_{440}	I_{604}/I_{440}
0 GPa	0.011	0.013	0.0009	0.0011
0.31	0.011	0.015	0.0009	0.0012
0.62	0.012	0.014	0.0010	0.0011
0.94	0.014	0.013	0.0011	0.0011
1.25	0.016	0.013	0.0013	0.0011
1.56	0.016	0.015	0.0013	0.0012
1.87	0.016	0.013	0.0013	0.0011
2.19	0.017	0.013	0.0015	0.0011

TECHNICAL REPORT DISTRIBUTION LIST, GEN

	<u>No. Copies</u>		<u>No. Copies</u>
Office of Naval Research Attn: Code 472 800 North Quincy Street Arlington, Virginia 22217	2	U.S. Army Research Office Attn: CRD-AA-IP P.O. Box 1211 Research Triangle Park, N.C. 27709	1
ONR Branch Office Attn: Dr. George Sandoz 536 S. Clark Street Chicago, Illinois 60605	1	Naval Ocean Systems Center Attn: Mr. Joe McCartney San Diego, California 92152	1
ONR Area Office Attn: Scientific Dept. 715 Broadway New York, New York 10003	1	Naval Weapons Center Attn: Dr. A. B. Amster, Chemistry Division China Lake, California 93555	1
ONR Western Regional Office 1030 East Green Street Pasadena, California 91106	1	Naval Civil Engineering Laboratory Attn: Dr. R. W. Drisko Port Hueneme, California 93401	1
ONR Eastern/Central Regional Office Attn: Dr. L. H. Peebles Building 114, Section D 666 Summer Street Boston, Massachusetts 02210	1	Department of Physics & Chemistry Naval Postgraduate School Monterey, California 93940	1
Director, Naval Research Laboratory Attn: Code 6100 Washington, D.C. 20390	1	Dr. A. L. Slafkosky Scientific Advisor Commandant of the Marine Corps (Code RD-1) Washington, D.C. 20380	1
The Assistant Secretary of the Navy (RE&S) Department of the Navy Room 4E736, Pentagon Washington, D.C. 20350	1	Office of Naval Research Attn: Dr. Richard S. Miller 800 N. Quincy Street Arlington, Virginia 22217	1
Commander, Naval Air Systems Command Attn: Code 310C (H. Rosenwasser) Department of the Navy Washington, D.C. 20360	1	Naval Ship Research and Development Center Attn: Dr. G. Bosmajian, Applied Chemistry Division Annapolis, Maryland 21401	1
Defense Technical Information Center Building 5, Cameron Station Alexandria, Virginia 22314	12	Naval Ocean Systems Center Attn: Dr. S. Yamamoto, Marine Sciences Division San Diego, California 91232	1
Dr. Fred Saalfeld Chemistry Division, Code 6100 Naval Research Laboratory Washington, D.C. 20375	1	Mr. John Boyle Materials Branch Naval Ship Engineering Center Philadelphia, Pennsylvania 19112	1

TECHNICAL REPORT DISTRIBUTION LIST, GENNo.
Copies

Dr. Rudolph J. Marcus
Office of Naval Research
Scientific Liaison Group
American Embassy
APO San Francisco 96503

1

Mr. James Kelley
DTNSRDC Code 2803
Annapolis, Maryland 21402

1

DTIC
ELECTE
DEC 19 1980
S D

TECHNICAL REPORT DISTRIBUTION LIST, 051A

	<u>No.</u> <u>Copies</u>		<u>No.</u> <u>Copies</u>
Dr. M. A. El-Sayed Department of Chemistry University of California, Los Angeles Los Angeles, California 90024	1	Dr. M. Rauhut Chemical Research Division American Cyanamid Company Bound Brook, New Jersey 08805	1
Dr. E. R. Bernstein Department of Chemistry Colorado State University Fort Collins, Colorado 80521	1	Dr. J. I. Zink Department of Chemistry University of California, Los Angeles Los Angeles, California 90024	1
Dr. C. A. Heller Naval Weapons Center Code 6059 China Lake, California 93555	1	Dr. D. Haarer IBM San Jose Research Center 5600 Cottle Road San Jose, California 95143	1
Dr. J. R. MacDonald Chemistry Division Naval Research Laboratory Code 6110 Washington, D.C. 20375	1	Dr. John Cooper Code 6130 Naval Research Laboratory Washington, D.C. 20375	1
Dr. G. B. Schuster Chemistry Department University of Illinois Urbana, Illinois 61801	1	Dr. William M. Jackson Department of Chemistry Howard University Washington, DC 20059	1
Dr. A. Adamson Department of Chemistry University of Southern California Los Angeles, California 90007	1	Dr. George E. Walraffen Department of Chemistry Howard University Washington, DC 20059	1
Dr. M. S. Wrighton Department of Chemistry Massachusetts Institute of Technology Cambridge, Massachusetts 02139			